An Automated System for Projection of Interior Construction Layouts

Amir Degani, *Member, IEEE*, Wen Bo Li, Rafael Sacks, Ling Ma

***Abstract*— Layout of the interior works during building construction is time-consuming and error-prone. Given the cost involved, both for initial layout and for later rework where errors occur, researchers have sought to automate the layout task. Some have adopted marker-less augmented reality (AR) methods using heads-up displays or cameras, and others have proposed robots capable of marking out the works. The former encumber the workers, the latter are expensive to set up and are sensitive to site conditions, and neither has yet achieved the required accuracy. In this work, we propose a more efficient approach to project relevant information from a Building Information Model (BIM) onto the construction surface, directly augmenting the construction site with the design information. This is done using a portable system consisting of a 2D laser scanner, an angled adjustable projector, and a camera. The system localizes itself within the already built outer walls using the laser scanner and the BIM model using a method derived from robotic mapping; it calibrates the projection correction parameters (keystone correction) using image analysis; and it projects the information with the angled projector. Testing results showed that the localization was accurate within a few millimeters and less than three degrees, and the final projected image's error was approximately one centimeter. Initial calibration requires less than one minute and does not require specialist skills. The system automates the layout task, preserves accuracy, and can provide rich model information on any interior surface.**

***Note to Practitioners*— Measuring and marking up of the interior works during building construction is time-consuming and error-prone. Layout must be repeated for each trade: partitions, false ceilings, mechanical, electrical and plumbing systems, flooring and furnishings all require accurate marking of locations on floors, walls and ceiling surfaces. Current automation is limited to the use of robotic total stations, but these only locate specific predetermined points. We propose a simple solution for automated layout, in which images from a building information model (BIM) are projected directly onto the work surface. The system projects any desired information – drawings, images, etc. – onto the work surface (floor, walls or ceiling) in the correct location, scale and orientation. The prototype apparatus consists of a laser range scanner, a projector, and a camera. Projection of the work instructions directly onto the work surface is accurate and immediate. It saves the time required for workers to interpret and then mark up the dimensional information and it avoids the human error involved. The prototype is limited to environments in which computer projection is practical and currently requires planar surfaces.**

***Index Terms*— Augmented reality, Automation in construction, Building Information Modeling, Construction site layout, Keystone correction, Localization**

I. Introduction

LAYOUT of the interior works during building construction is time-consuming and error-prone. Builders must interpret the drawings relative to the interim reality of the structure and any works in progress, and then make measurements to place the next stage of work. Layout must be repeated for each trade: partitions, false ceilings, mechanical, electrical and plumbing (MEP) systems, flooring and furnishings all require accurate marking of locations on floors, walls and ceiling surfaces.

Although no industry-wide data have been published defining the labor consumption for marking up[1], the scale of direct effort and subsequent rework in case of error have prompted many research and development efforts to build automated layout systems. Three types of systems have been proposed:

a) Augmented reality (AR) systems, in which an image of the intended design is superimposed onto an image of the site recorded with a camera [1]–[3];
b) Layout marking robots, in which a robot localizes itself and then travels the work area applying paint or other marking material directly onto the surface [4], [5];
c) Robotic Total Station (RTS) survey layout, in which an operator uses a marker to identify layout points by sighting a target reflector from the total station [6].

Each of these systems has limitations; AR systems require the user to wear special glasses or masks, or to hold up a mobile computer or other device on which the images are projected. The user must then translate that information onto the work surface. These systems are proving to be useful for building or facility operation and maintenance tasks [7], for example where

Submitted for review 6 September, 2016,

A. Degani is with the Division of Environmental, Water and Agricultural Engineering, Faculty of Civil and Environmental Engineering, Technion – Israel Institute of Technology, Haifa 32000, Israel +972-4-8292632, (email: adegani@technion.ac.il), corresponding author.

W. B. Li is with the Faculty of Applied Science and Engineering, University of Toronto, Toronto, Ontario M5S2E4, Canada, mailwen.li@mail.utoronto.ca

R. Sacks is with the Division of Structural Engineering and Construction Management, Faculty of Civil and Environmental Engineering, Technion – Israel Institute of Technology, Haifa 32000, Israel +972-4-8293190 (email: cvsacks@technion.ac.il).

L. Ma is with the School of Art, Design and Architecture, University of Huddersfield, Huddersfield HD1 3DH, UK +44 (0) 1484 473589 (email: l.ma@hud.ac.uk). He was a postdoctoral researcher at Technion when he was involved in this research.

[1] Trimble and DPR Construction reported measuring marking up of drywall partitions in a hospital building at the rate of approximately 130-150 linear feet of layout per hour when done using tape-measures, chalk, and laser pointers [4].

MEP systems hidden from view behind walls or ceilings can be observed on the backdrop of the existing material. Although they are useful during construction for conveying information other than geometry about components that are to be installed or checked, they are not practical for the initial layout.

Robotic marking systems are restricted to environments where the floors are clean and clear, for marking and for travel, and where the quantity of layout work is large enough to justify their setup costs. To date no commercial systems are available. RTS layout, on the other hand, has become commercially viable and is used particularly for layout of MEP systems before concreting or for setting points for formwork. The primary limitations are that only points can be marked out, that clear lines of sight must be maintained between the RTS and the target points, and localization of the RTS requires visible survey points and/or GPS access. It is not a practical solution for workers in relatively confined and enclosed spaces, it requires a specialist operator, and it cannot provide any information other than point locations.

Adopting a hybrid approach, we propose a simple technological solution for automated layout in which images from a building information model (BIM) [8] are projected directly onto the work surface (shown in Fig. 1 in a proof-of-concept experiment). The system uses information of the existing geometry to help determine its location, and then uses images of the layout to project the correct image directly onto the floor, similar to methods done in spatial augmented reality [9]. The prototype apparatus consists of a 2D range scanner - LiDAR (Light Detection And Ranging), an angled adjustable projector, and a camera. The system performs three steps: 1) it localizes itself within the already built outer walls using the LiDAR and the BIM model using a method derived from robotic localization; 2) it calibrates the projection correction parameters (keystone correction) using image analysis; and, 3) it projects the information with the angled projector.

To achieve accurate and automatic projection, the method employs a LiDAR device localization algorithm and an automatic keystone-correction projection algorithm which itself consists of a projection method and a calibration method. The localization and calibration methods determine the area in the workspace onto which the projector will project; the projection method then corrects the keystone effect[2], referred to as oblique projection in [9], that arises due to the slanted projection of images. These algorithms work together to ensure an accurate display of the layout image.

After presenting existing research and systems, the following sections of this paper present the research prototype, the algorithms used, and the results obtained from its operation in an experimental environment. Two proof-of-concept experiments are presented: a small mockup environment to accurately measure the errors in the three stages: localization, calibration, and projection, and a second experiment in a large office. This final proof-of-concept experiment was meant to show the system performing in a full-scale environment.

Fig. 1. Overview of the system in a proof-of-concept experiment of a bathroom layout projected on the floor. The system is composed of a laser scanner to localize itself in the room; an angled projector then projects the relevant information on the construction surface. When the system is moved to a new location, it automatically re-localizes itself in seconds and projects the accurate and updated design information. The system is first calibrated to calculate how to pre-warp the image in order for the image to be precisely projected on the

II. Related work

As outlined in the introduction above, research and development efforts aimed at automating construction layout has resulted in systems that can be broadly classified as one of three types: AR systems, layout marking mobile robots, and RTS survey layout. Although the latter is limited to the layout of individual marker points and requires line of sight between the survey station and the marking pole used to determine the locations, RTS is the only one of the three currently used in everyday practice. The following sub-sections review the application of AR in construction in general and for layout in particular, layout marking robots, and identify the lack of AR systems that are quick to set up and do not encumber users.

A. Augmented Reality Applications in Construction

With the rapid development of AR technology and specifically in projection-based AR [9], opportunities also emerge in the construction industry for exploiting AR for various applications [2], [3]. AR systems can increase the efficiency and quality of construction work by providing digital content on top of physical background views to assist construction workers. These systems fall within broad categories and can benefit many construction processes by providing 2D images, 3D objects and/or data, texts, or indicators [10]. They can provide information about components that either have not yet been installed or that are hidden by subsequent layers of material, and can therefore support a wide range of operations (such as layout, fabrication and installation, quality control and facility maintenance). They function by reducing the time required for the original operations and/or the probability of rework by removing the

[2] Usually "keystoning" refers specifically to a symmetric, trapezoidal distortion caused by projector vertical misalignment. In this work, the term refers to the broader class of distortions creating a non-symmetric quadrilateral shape that occurs from an off-axis projection in both the vertical and the horizontal axes.

chance of an error due to misinterpretation of information.

Koch et al. [11] presented an AR-based system for navigating and instructing facility operators to perform maintenance tasks. Hou et al. [12] demonstrated the effectiveness of using AR to guide assembly tasks based on controlled experiments with LEGO models. Yang and Ergan [13] demonstrated the benefits of encoding semantic information with visualization techniques for facility operations in the building environment where the operator often loses the spatial context, showing how semantic information can be easily extracted from a BIM model and integrated into an AR system, which provides a user-friendly visualization interface [14]. The synergy of using BIM and AR in construction projects has been demonstrated in different scenarios, such as context-aware onsite navigation [15], piping assembly instruction [16], situation-aware facility management [7], [17] and on-site detection of construction defects [18]. Williams et al. [19] proposed a detailed workflow for translating BIM models for use in a mobile AR platform, thus setting the stage for the direct use of BIM information through AR on site. Their pilot study in facility management revealed that BIM model localization and target registration are the primary challenges to the use of BIM models within AR applications [19]. Daponte et al. [20] also emphasized that the effectiveness of AR application depends highly on the accuracy of the calibration system for target tracking.

Shin and Dunston [21] analyzed the human factors of a variety of construction tasks to identify those application areas that might benefit from AR technology. Layout was one of the eight application areas identified as most suitable.

B. Layout Marking Mobile Robots

A number of research projects have developed and tested mobile robotics to solve the problem of marking the layout at a construction site. Tanaka et al. [22] reported the development of a machine to mark points for MEP system hangers on ceilings, intended to replace the tedious, slow and dangerous manual work required to locate and drill marker holes. In 1995, a US patent was granted for a 'Navigating robot with reference line plotter' that was intended for marking out construction works [23]. A more recent patent application [5] describes a similar system but with the addition of a geo-referenced base station which guides the marking robot. Although computer simulations [24] and a prototype [4] demonstrate the concept of robots drawing the layout of interior works on the concrete floor surfaces of buildings under construction clearly, accurate localization of the robots and the operational setup cost for using such robots are challenges that must yet be overcome before they become sufficiently accurate and commercially viable.

Both the AR and the robotic layout approaches suffer from drawbacks that hamper their implementation in industry. The AR methods without markers have yet to achieve the necessary accuracy and they encumber construction workers, which is a significant drawback in inherently awkward and/or unsafe construction site environments. Robotic applications, just like other construction robot applications, carry the burden of very high setup costs that must be offset by large work volumes in clean and accessible locations [25]. Thus, a gap exists for a solution that provides AR information with minimal setup and without requiring users to hold or wear any equipment. This is the gap filled by the proposed solution.

C. Localization and Keystone Correction

The localization portion of this project is similar to a static robotic mapping problem. Though robotic localization problems most commonly refer to mobile robotic localization, the static problem can be thought of as a particular step in the mobile localization problem during which the robot is stationary.

One of the existing methods for robotic localization is Monte Carlo Localization (MCL) [26]. MCL is used for the localization of mobile robots, and uses data from odometry sensors (e.g., wheel encoders) and distance sensors (e.g., LiDAR) to find probable poses of a robot in a given configuration space (C-Space). This method analyzes the probability of random poses and updates their values and probabilities with both sensor and movement data through successive iterations to acquire the live pose of the robot as it moves in the C-Space. The iterative and probabilistic nature of MCL makes it efficient and accurate for complex problems such as mobile localization.

Another robotic localization algorithm that is closer to the actual current implementation is Markov Localization (ML) [27], which attempts to localize a moving robot within a static environment. It does so by dividing the C-Space into a grid, and finds the probability of the robot being present in each grid space given a measurement from the odometry and distance sensors. This process is done over successive iterations to output likely poses at a new time.

In our work, after the localization phase, the system projects the scene on the desired plane (floor or wall). Previous works have also arrived at automated solutions to the problem of correcting an image projected at an angle to the projection surface. The solutions, which are called automatic keystone correction algorithms, focused on correcting the image from a visual presentation (e.g., PowerPoint presentation) without manual input [28]. The method first identified the transform needed to pre-distort the projected image, which, when projected, exactly cancels the physical distortion; afterwards, the largest rectangular shape is identified from the projected area, and the keystone corrected image is displayed. Several more general (and spatial) methods are mentioned in [9].

III. MATERIAL AND METHODS

A. Apparatus

The proof-of-concept prototype depicted in Fig. 3 consists of a LiDAR (URG-04LX; Hokuyo Automatic Co., ltd., Japan), a portable projector, a webcam (Logitech, USA), a mount which allows the projector's angle to be adjusted, and a laptop computer for controlling the system. The LiDAR is capable of measuring between 0.02m and 4m at 240° with a manufacturer's stated accuracy of ±0.01m, an angular accuracy of 0.36°, and a frequency of 10Hz. However, in our setup, we

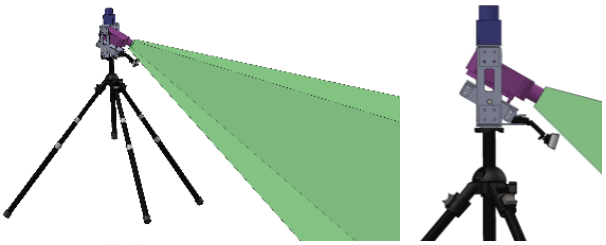

Fig. 3. Proof-of-Concept Apparatus. Left: Isometric view, right: side view. The Hokuyo URG-04LX LiDAR is positioned on top to scan a horizontal plane parallel to floor, the projector is mounted at an angle toward the floor, and the camera, which is only used for the calibration process, is mounted at an arbitrary position viewing the projection on the floor.

have averaged each scan over 40 samples and, in our experimental setups, reached an accuracy of ±0.002m, similar to [29]. This system was first tested in a small mockup environment with dimensions of approximately 1.0 m by 1.4m (shown in Fig. 5), and later in a large office (shown in Fig. 11). For the small-scale experiments, described in sections IV.A-IV.D, we used a simplified tripod to allow the laser to operate effectively. In the final, large-scale proof-of-concept in section IV.E, a full tripod, as shown Fig. 3, was used to demonstrate the capabilities in a larger room.

B. Methods

1) System operation overview

The proof-of-concept system operates in three steps shown in Fig. 3. The construction-site worker places the system in the vicinity of the working area. Given the BIM model of the already built outer walls, the system first localizes itself using the LiDAR (Algorithm 1). Then, the system projects the desired image on the surface of interest, which could be partitions, false ceilings, mechanical, electrical and plumbing systems, flooring and furnishings projected on floors, walls, or ceiling surfaces. Since the projector is mounted at an angle relative to the surface, the image must be pre-warped before projection. In order to correctly warp the image, the system must acquire the transformation between the projector and the surrounding. We provide a calibration algorithm (Algorithm 2) to accurately find this transformation. Finally, the corrected image is projected on the surface at the specific region of interest (ROI).

1) Localization

First, the system must find its pose accurately. Similar to Markov Localization (ML) [27] described above, Algorithm 1 attempts to localize and find the most probable pose (MPP) given the existing walls vertices and a laser scan. In summary, the static localization algorithm first discretizes the C-Space, that is, locations and orientations (step 1). For each pose in the grid, the algorithm calculates the difference between the distances measured by the LiDAR and the theoretical LiDAR readings, had it been positioned at that pose (step 2). A multi-start optimization function is invoked to find all local minima of the sum of square of errors (SSE) under a specified threshold

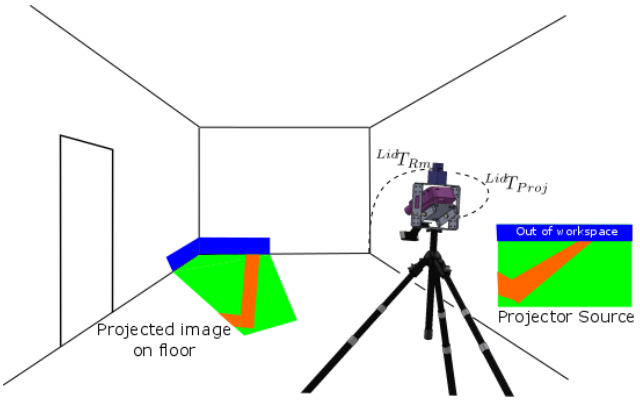

Fig. 2. System operation overview. The system first localizes itself relative to a known map to find $^{Lid}\boldsymbol{T}_{\boldsymbol{Rm}}$ (Algorithm 1). The system then uses the calibration algorithm (algorithm 2) to find the transformation between the room, the LIDAR and the projector ($^{Lid}\boldsymbol{T}_{\boldsymbol{Proj}}$) to correctly pre-warp the image so it projects correctly on the floor.

(step 3). If only a single MPP is found, it is returned (step 4).

Additionally, there would be cases where ambiguities exist, i.e., two poses that perfectly match the LiDAR scan (imagine a rectangular room where there are always two antipodal ambiguous poses). At this stage, there are two ways of identifying the correct MPP. Since the LiDAR used in the experiment only covers 240°, one way of eliminating incorrect MPPs is by rotating the system and analyzing again the errors of the ambiguous MPPs (step 5.1.1). However, because symmetric perspectives (e.g., a perfectly square room) are indistinguishable from each other, not all ambiguities can be eliminated using this method. The second option to identify the correct MPP is through manual identification where the user is asked to input which of the MPPs is the correct one (step 5.1.2).

Algorithm 1 - Projector Localization

Input: wall vertices (v), LiDAR scan (d), *grid size*, *grid resolution*, *error threshold*, *pose tolerance*
Output: Most probable pose (MPP)

1. Divide C-Space into pose grid with *grid size* and *grid resolution* (*param*) (number of poses (p) is *N).*
2. **For** each pose (p) in the grid
   2.1. Get error of the pose using ***CalculateSSE***: $E_N = CalculateSSE(v, p, d)$ and insert all MPPs into C_i.
3. **For** all candidate MPPs in C_i,
   3.1. Update C_i by finding the set of unique local minima poses lower than the *error threshold* using the multi-start method ***MultiStart***[3]. Uses *pose tolerance* parameter to distinguish between nearby poses.

   Note: At this point, C should only contain non-adjacent minima in the original grid function
4. **If** C has only one element
   4.1. **Return** the candidate as the MPP.
5. Else[4]
   5.1. Get user input
      5.1.1. **If** user chooses to rescan with LiDAR in different orientation
         5.1.1.1. Rescan with LiDAR to get new d.

[3] "*MultiStart*" finds multiple local minima using multiple starting points. Part of the Global Optimization Toolbox of MATLAB™

[4] Continuous mode of operation, where the user constantly moves the system nearby, will not prompt user input after the first iteration of the Projector Localization algorithm, instead, the MPP in C closest to the pose of the previously calculated MPP is returned as the new MPP.

5.1.1.2. **Go to** step 4 with C as C_i (i.e., the remaining ambiguous MPPs).
5.1.2. **Else if** user chooses to select correct MPP manually
5.1.2.1. **Return** the selected MPP

Sub-algorithm 1.1 - CalculateSSE

Input: wall vertices (v), LiDAR scan (d), pose (p)
Output: SSE between LiDAR data if LiDAR were situated at pose p and its actual position within existing walls.

1. **If** pose is not contained inside existing walls
   1.1. Return NaN[5]
2. **For** each scanning laser of the LiDAR
   2.1. **For** each wall of the existing walls
      2.1.1. Get the point of intersection (POI) between the wall and the laser
   2.2. Remove POIs in opposite direction as the laser ray
   2.3. Get the remaining POI closest in distance to p

Return the sum of squares of all such POI to p distances

2) Calibration

When the system projects an image at an angle toward a planar surface, it undergoes a distortion (sometimes called the keystone effect). Our motivation is to perform a calibration using a camera so that the system can pre-warp the image in order for the image on the floor to show correctly. This is typically done only once during setup and will not be executed when the system is moved around the construction site.

The calibration method is summarized in Algorithm 2 and Fig. 4. This method is based on a similar method for automatic keystone correction [28], [30] and also in chapter 5 in [9]. The goal is to find the transformation between the projector and the LiDAR so the image can be correctly pre-warped as described in projection method. In order to achieve the desired transformation we use a camera as a middle step.

The steps of the method are as follows:

1. Localize the system to find the position of the LiDAR within the room (the workspace) to find ${}^{Lid}T_{Rm}$, where T denotes the homogeneous transformation.
2. Place a jig (in our case a white rectangle inside a larger rectangle) at a known location in the room, e.g., top left corner. This provides us the transformation ${}^{Rm}T_{Jig}$.
3. The camera acquires an image of the rectangle jig and extracts the four vertices in the image in the Cam-Space $({}^{Cam}T_{Jig})$.
4. By chaining the above transformations, we find the transformation between the Cam-Space and the pose (LiDAR): ${}^{Lid}T_{Cam} = {}^{Lid}T_{Rm}\ {}^{Rm}T_{Jig}\ {}^{Cam}T_{Jig}^{-1}$.
5. Next, we project a virtual rectangle onto the floor, and as before, extract the positions of the vertices of the projected area from the Cam-Space.
6. Using the homographic projection (explained next), we find the transformation between the projector and camera$({}^{Cam}T_{Proj})$.
7. From the transformations of steps 4 and 6, find the desired final calibration transformation $({}^{Lid}T_{Proj} = {}^{Lid}T_{Cam}\ {}^{Cam}T_{Proj})$. Since we have already localized in Step 1, we also have the transformation between the projector and the workspace $({}^{Rm}T_{Proj})$.

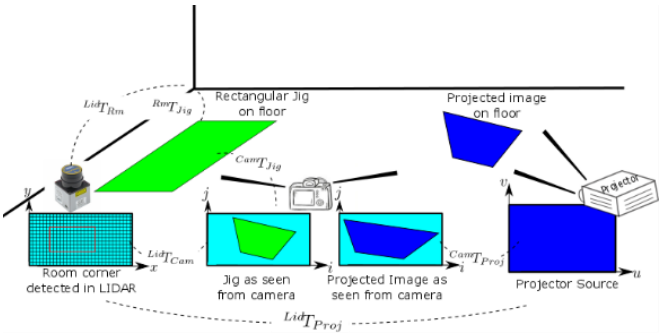

Fig. 4. Calibration procedure. The end result of the calibration is to find the transformation between the Projector and the LiDAR ($^{Lid}\boldsymbol{T}_{\boldsymbol{Proj}}$). Left: The system uses Algorithm 1 localization to find($^{Lid}\boldsymbol{T}_{\boldsymbol{Rm}}$). A camera acquires the rectangular jig on the floor ($^{Cam}\boldsymbol{T}_{\boldsymbol{Jig}}$). The Jig is placed on the floor near a corner of the room. The Jig is designed such that the location of the rectangle is known relative to the room's corner (denoted $^{Rm}\boldsymbol{T}_{\boldsymbol{Jig}}$). By using Algorithm 1, the LiDAR is localized relative to the room ($^{Lid}\boldsymbol{T}_{\boldsymbol{Rm}}$). Chaining these transformation, we arrive at ($^{Lid}\boldsymbol{T}_{\boldsymbol{Cam}} = {}^{Lid}\boldsymbol{T}_{\boldsymbol{Rm}}\ {}^{Rm}\boldsymbol{T}_{\boldsymbol{Jig}}\ {}^{Cam}\boldsymbol{T}_{\boldsymbol{Jig}}^{-1}$). Right: a rectangle is projected on the floor and the camera captures this image and the homography from projector to camera.

In step 5, we project a rectangle from the projector source onto the floor creating a trapezoid. Consider a point (u, v) in the projector source. This point is projected to some unknown point on the floor (by a perspective transform whose parameters depend on the unknown position and orientation of the projector and the unknown focal length of the projector optics). The four trapezoid vertices on the floor are then observed by the camera at pixel location (i, j) (undergoing a second perspective transform whose parameters depend on the unknown position and orientation of the camera relative to the screen, and the unknown focal length of the camera optics). Our goal is to recover the mapping between (u, v) and (i, j). We exploit the fact that the four observed vertices lie on the planar floor that establishes a homography between the camera and projector frames. Thus, the compounded transforms mapping (u, v) in the projector frame, to some unknown point on the floor, and then to pixel (i, j) in the camera frame, can be expressed by a single projective transform,

$$(u, v) = \left(\frac{h_1 i + h_2 j + h_3}{h_7 i + h_8 j + 1}, \frac{h_4 i + h_5 j + h_6}{h_7 i + h_8 j + 1}\right), \quad (1)$$

or similarly, in homogeneous coordinates matrix form as

$$\begin{pmatrix} uw \\ vw \\ w \end{pmatrix} = \begin{pmatrix} h_1 & h_2 & h_3 \\ h_4 & h_5 & h_6 \\ h_7 & h_8 & 1 \end{pmatrix} \begin{pmatrix} i \\ j \\ 1 \end{pmatrix}, \quad (2)$$

with eight degrees of freedom of the homography matrix $\vec{h} = (h_1, \dots, h_8)^T$. By using four distinct and non-collinear vertices of the rectangle projecting to a trapezoid and acquired as another trapezoid by the camera, and by converting to matrix form, we arrive at the 8×8 matrix

[5] NaN (Not a Number in MATLAB) as an invalid number is returned for invalid poses so that in both Candidate MPP Detection (Sub-algorithm 1.1) and pattern search algorithms (see Algorithm 1), none of these poses are later selected as MPP in C.

$$\begin{pmatrix} i_1 & j_1 & 1 & 0 & 0 & 0 & -i_1u_1 & -j_1u_1 & -u_1 \\ 0 & 0 & 0 & i_1 & j_1 & 1 & -i_1v_1 & -j_1v_1 & -v_1 \\ i_2 & j_2 & 1 & 0 & 0 & 0 & -i_2u_2 & -j_2u_2 & -u_2 \\ 0 & 0 & 0 & i_2 & j_2 & 1 & -i_2v_2 & -j_2v_2 & -v_2 \\ i_3 & j_3 & 1 & 0 & 0 & 0 & -i_3u_3 & -j_3u_3 & -u_3 \\ 0 & 0 & 0 & i_3 & j_3 & 1 & -i_3v_3 & -j_3v_3 & -v_3 \\ i_4 & j_4 & 1 & 0 & 0 & 0 & -i_4u_4 & -j_4u_4 & -u_4 \\ 0 & 0 & 0 & i_4 & j_4 & 1 & -i_4v_4 & -j_4v_4 & -v_4 \end{pmatrix} \begin{pmatrix} h_1 \\ h_2 \\ h_3 \\ h_4 \\ h_5 \\ h_6 \\ h_7 \\ h_8 \end{pmatrix} = 0. \quad (3)$$

Solving the system of linear equations (3), we arrive at the desired homography transformation, ${}^{Cam}T_{Proj}$. Moreover, finding the transformations from step 3 in a similar fashion, allows us to find the desired transformation, ${}^{Lid}\boldsymbol{T}_{\boldsymbol{Proj}} = {}^{Lid}\boldsymbol{T}_{\boldsymbol{Cam}}\,{}^{Cam}\boldsymbol{T}_{\boldsymbol{Proj}}$. This finally allows us to pre-warp the image while projecting the desired construction layout described in the next section.

Algorithm 2 - Projector Calibration Parameter Calculation

Input: wall vertices (*v*), Most probable pose (MPP), Camera image of calibration: rectangle (*rectI*), keystone (*keystoneI*), region growing tolerance (*tol*)

Output: Positions of vertices of the projected image with respect to position of LiDAR

1. Get the binary image of $rectI$ using a region growing algorithm according to tolerance tol**.**
2. Get the positions of the vertices of the binary image using **getPoints**[6].
3. Solve the projective transformation formula using v and the vertices of the binary image. This derives the transformation, T, between the Cam-Space and workspace.
4. Get the binary image of $keystoneI$ using a region growing algorithm according to tolerance tol.
5. Get the vertices of this binary image using **getPoints**.
6. Get the vertices of the keystone in C-Space by using T.
7. **Return** the relative pose between keystone and MPP.

3) Projection

The projection method consists of two steps: Identification of projected space region of interest (ROI) and the pre-warping of the projected image to correct for the keystone effect. In the first step, the quadrilateral section of the map onto which the projected space reaches is determined. Since the transformation ${}^{Lid}T_{Proj}$ is known from the previous calibration process and knowing the MPP, the system identifies the projected space ROI on the map of the room.

As explained in the previous section, since the projector is placed at an angle to the floor, a projection of what is on the rectangular computer screen undergoes the keystone effect whereby different parts of the same image are variably stretched, distorting the image. Thus, in the second step, a pre-warping transformation is applied to the ROI image, which exactly cancels the keystone effect, projecting the exact image as seen in the original quadrilateral section.

IV. Results

We present results from two proof-of-concept experiments. The first was a small mockup environment (shown in Fig. 5). A sheet of millimeter graph paper was affixed to the floor to accurately measure the errors in the three stages: localization, calibration, and projection. The second experiment was done in a large office (shown in Fig. 11). This final proof-of-concept experiment was meant to show the system performing in a full-scale environment.

A. Localization

We tested the localization algorithm in a small-scale room mockup (1 m by 1.4 m) as shown in Fig. 5. Sixty measurements were conducted, one for each combination of three parameters: four poses in the x-direction, five poses in the y-direction, and three orientations (-45°, 0°, 45°). Ten impossible configurations were omitted since they were too close to the walls. We placed the apparatus in these locations, used the localization algorithm to detect the MPP, and compared to the known location. The mean error in the x-direction, y-direction, and orientation, from all 50 poses were found to be 5.7 mm, 5.9 mm, and 2.5°, with a standard deviation of 3.4 mm, 4.6 mm, 0.5°, respectively. Fig. 6 depicts the localization errors in the 50 poses. To portray how the localization error changes with location, we plot error rectangles where the lengths of the edges are five times larger than the error between the MPP and the "ground-truth" in each pose in the x-, and y-direction. The least accurate results occurred in the poses where the apparatus was very close to a wall, and hence the LiDAR was at its limit. When the system is farther away from the wall, the precision is higher. If only the middle eight poses, which are at least 400 mm away from the walls are analysed, the mean error in the x-direction, y-direction, and orientation, decreases to 3.6 mm, 3.6 mm, and 2.5°, with a standard deviation of 1.8 mm, 3.3 mm, 0.6°, respectively, well under 10 mm mean error, which suffices our precision need.

B. Calibration

The calibration accuracy was tested by projecting a square immediately after calibration and without moving the system,

Fig. 5. Localization verification experiment. Experiment for testing the localization algorithm. Sixty measurements were conducted in a 1 m x 1.4 m room mockup. Four poses in the x-direction, five poses in the y-direction, and three orientations (-45°, 0°, 45°).

[6] **getPoints** is a vertex-extracting algorithm.

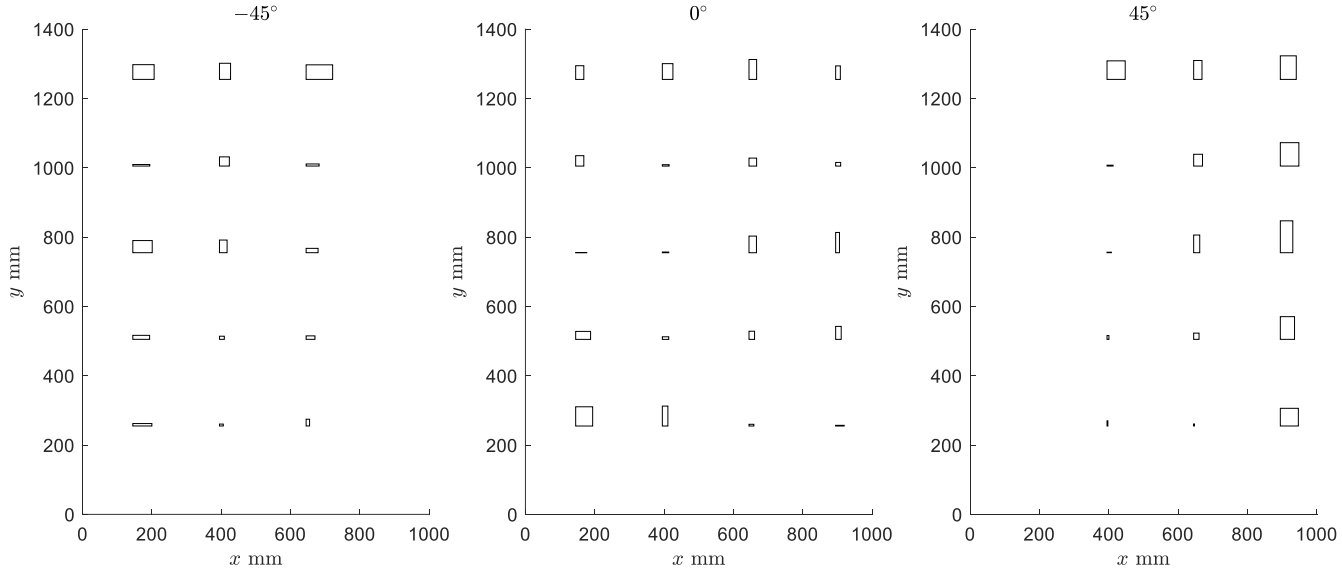

Fig. 6. Localization verification. Error of the predicted pose (MPP) at different locations using three orientations: left:−45°, middle: 0°, right: 45°. Blank areas in left and right figures represent impossible configurations of system since they were too close to wall. Size of rectangles are five times larger than the localization errors.

which bypasses localization errors. The projection of the four vertices was accurate to within 1 mm. The speed of calibration depends on how quickly the system can be set up at the construction site. In our tests calibration was usually done within a minute.

C. *Projection*

As long as the resolution of the projector is high and it has a large depth of focus, there are no errors when images are transformed from one projective space to another, meaning that if there were neither localization error nor calibration error, the projection would be perfect. However, when localization errors and calibration errors are introduced together with the fact that in our system the projector has a short depth of focus, the projection error increases as the localization error increases. In the conclusion section, we discuss possible ways to reduce these errors.

In our mockup room tests, we positioned the system in the bottom eight poses shown in Fig. 5 (similar to the tests done in Fig. 6b) and projected a 0.1 m x 0.1 m square onto the floor. We then measured the error of the four vertices of the projected squares, depicted in. Fig. 7. Mean error of each projected square is indicated mid-square. The mean error of all vertices was 6.6 mm with 2.9 mm standard deviation.

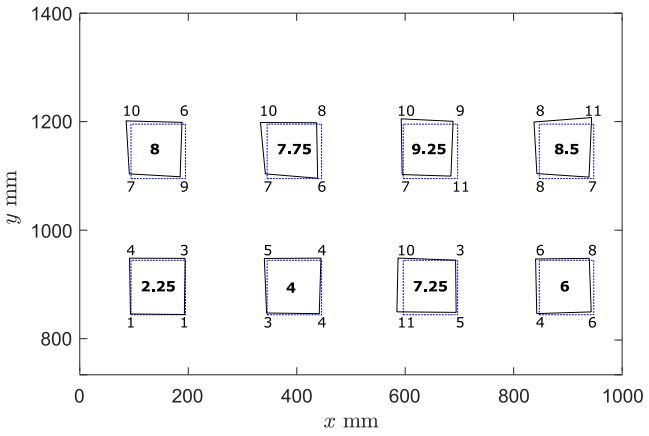

Fig. 8. Projection verification. Eight square projections are shown. Dashed lines represent the desired projected square. Black polygons qualitatively represent the true projection. The error of each corner is presented near the corresponding corner. Average error is presented mid-square.

D. *Small-scale proof-of-concept experiment*

A small-scale proof-of-concept experiment was conducted to validate the integration of the localization, calibration and projection. The same mockup room test as in the previous sections was used. A simple layout of a room, shown in Fig. 8, with a small cabinet (approximately 0.4 m x 0.4 m) at the North-West corner, and a toilet at the North-East corner, were projected on the floor. Fig. 9 depicts eight snapshots from the experiment showing the full process of localization and projecting the relevant image onto the floor. Each time the system was moved, it automatically localized itself and projected a new corrected image in under five seconds. We measured the error of the projected image using the millimeter

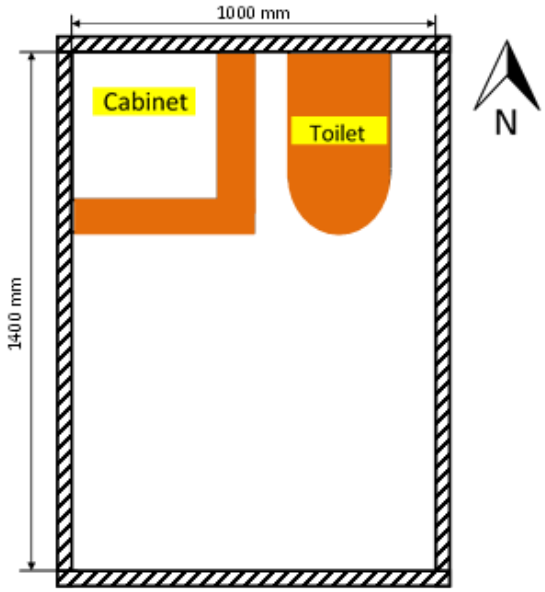

Fig. 7. Layout used for small-scale proof-of-concept experiment.

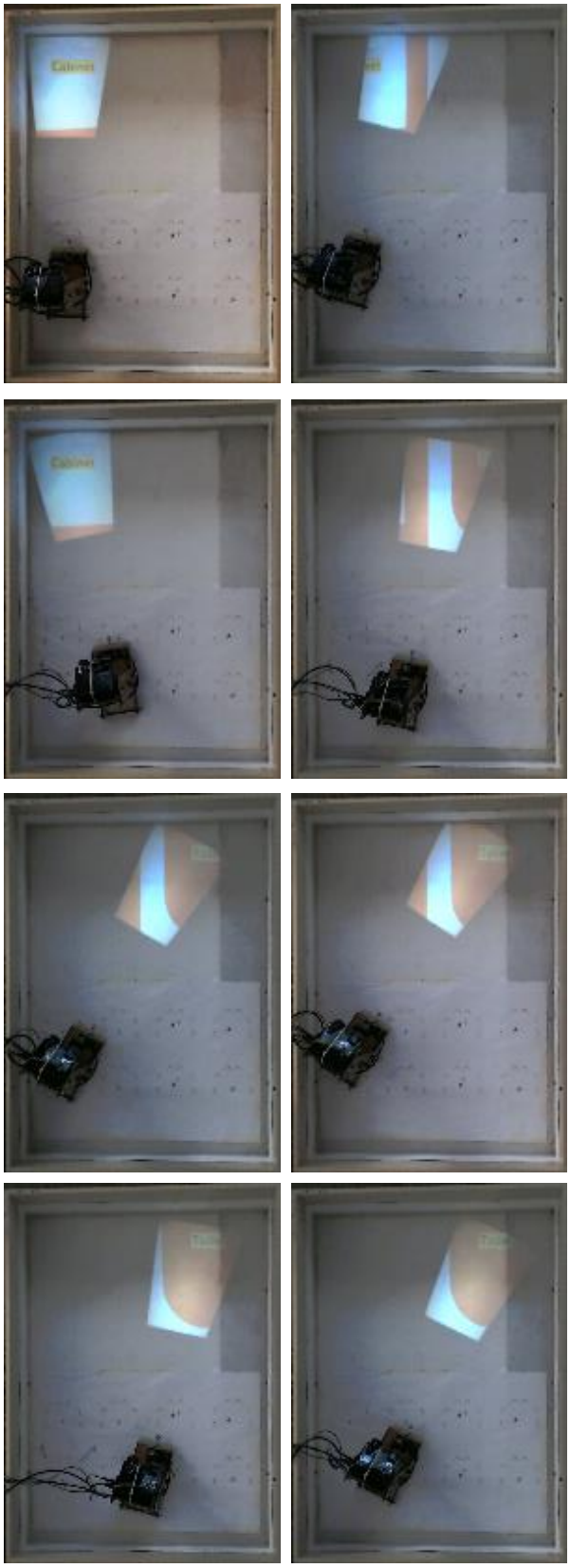

Fig. 9. Small-scale proof-of-concept experiment. In the mock-up room we projected a floor plan with a small cabinet (approximately 0.4m x 0.4m) – North-West corner of the room, and a toilet – North-East corner of the room. Eight snapshots from the experiment show the full process of localization and projecting the relevant image onto the floor. Each time the system was moved, it automatically localized itself and projected a new corrected image in under five seconds.

paper on the floor, and found that the average maximum error was less than 10 mm with a maximum of 15 mm deviation in one case.

E. Large-scale Proof-of-concept experiment

For the final proof-of-concept, the system was used in a regular sized office (approximately 3.8 m x 2.8 m) to demonstrate the prototype capabilities. We projected a typical bathroom layout (shown in Fig. 10) on the office floor. Fig. 11 depicts eight snapshots of the apparatus after it was moved to different poses. Unlike the small-scale proof-of-concept experiment where we were able to accurately draw the "ground truth" on the millimeter paper, in this experiment we measured the difference in the location of the region the system expected to project outside the floor (blue in the projection). In these experiments, we have found a maximum error of 12 mm. As with the case of the small-scale experiment described above, each time the system was moved, it automatically localized itself and projected the new corrected image in under five seconds.

V. Discussion and Possible Improvements

The current prototype works well in the small testing ground and the full-scale bathroom mock-up used in the experiments, but would require improvement before use in a building under construction. The following outlines the potential benefits, limitations and possible solutions.

Notwithstanding the technical improvements needed, the relevance and value of this research lie in its proposal of a new approach to the challenge of automating site layout in construction. The proposed system has advantages when compared with all three existing approaches to marking up work on site – the commercial RTS systems, the experimental layout marking mobile robots, and the augmented reality systems. It is more efficient than an RTS because it does not require a specialist operator nor preparation of the information in the office before coming to a site. It also can be used in closed and in confined spaces, such as tiling layouts in bathrooms or electrical system layout in interior rooms where the use of an RTS is impractical. Unlike a layout marking mobile robot, it does not require a flat, clear surface to move on and it is more accurate than existing robot prototypes. It can also project on walls or other planar surfaces. An important advantage is that it can convey far more information and far more quickly than either RTS or layout marking robots, because the image projected is rich in graphics, and the image can contain text as well. The images can be tailored to match the stage of production, and they may include animations. Photographs of earlier working conditions can also be used, for example, where the need arises to identify the locations of ducts or pipes that have been covered. When compared with augmented reality solutions, other than accuracy, the other main advantages are that the users are not required to wear or hold any equipment that may interfere with their normal working pose and ergonomics, translation of the information onto the work surface is direct, and setup is quick and automatic, allowing workers to move the equipment as they move.

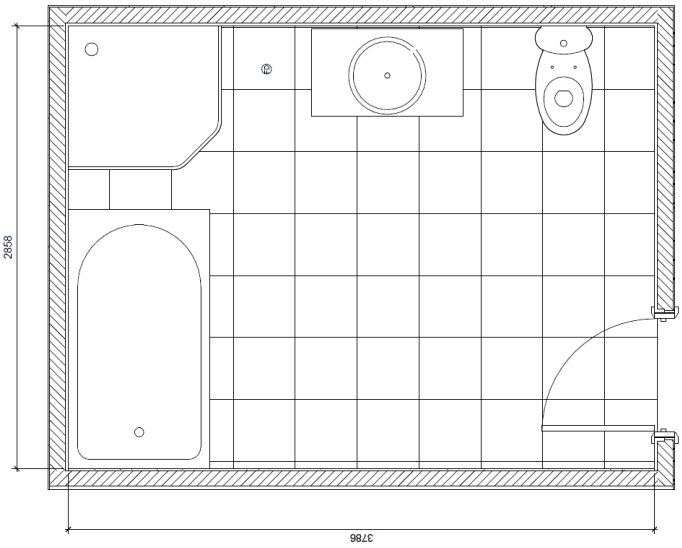

Fig. 10. Bathroom layout used for large-scale proof-of-concept experiment

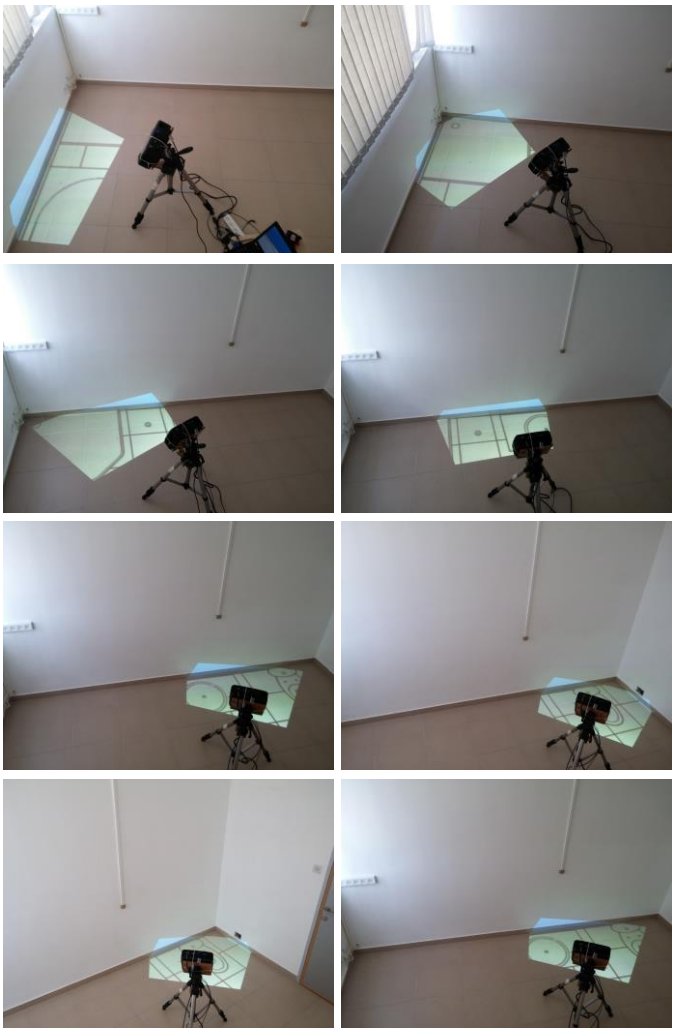

Fig. 11. Large-scale proof-of-concept experiment. A bathroom layout (shown in Fig. 10) was projected on the floor. Snapshots from the experiment show the full process of localization and projecting the relevant image onto the floor. As can be seen, as the apparatus is moved it re-localizes itself and projects the correct image on the floor. The localization and projection at each new position is done automatically in under five seconds.

While the current prototypes may already provide the accuracy needed for certain facility operations and maintenance tasks, improvements are needed before performing long-term tests on a construction site. Firstly, a LiDAR unit with greater range and accuracy than the small unit used in the prototype is needed (such units are readily available). The current system produces localization (positioning) errors and final projection errors of up to 10 mm. To reduce the outliers sensed by the LiDAR, we intend to implement an algorithm which recognizes the existing walls using algorithms such as RANSAC. The resulting improvement in accuracy could reduce the cost of such systems by reducing the accuracy requirements of the LiDAR. This improvement would also allow the projection step to be done with better precision.

Secondly, the projector calibration can be done more accurately and with more ease if the camera were placed at a higher static position overlooking the projection area. The camera should only have to be calibrated once, and the system could be easily calibrated at any place in the work area. Of course, this entire calibration can be replaced by an accurate mechanical measuring device (e.g., encoders) on the tripod which will form the required transformations. Moreover, a 2-D laser projection system could reduce the inaccuracies that arise from out of focus areas at the edges of the images on the surface. A multi-projector layout, [9], could also be deployed to increase the projected image on the scene. Finally, depth sensors or a patterning technique for sensing the inaccuracy in floor shape, could potentially further reduce errors caused when projecting on complex, non-planar surfaces, in a fashion similar to that presented in [9], [31].

Nevertheless, despite the limitations of the prototype, this novel approach holds the potential for development of low-cost automatic systems which could not only increase the speed of marking up a layout for construction work, but also provide far richer information more reliably and naturally than is possible with other methods.

As the technology is developed, further research will also be needed to establish suitable modes of work with the tool. For example, discrepancies between actual conditions ‘as-built’ in the field and the ideal locations and dimensions of objects as defined in design documents are a common occurrence in construction, whether designs are prepared with traditional 2D drawings or with BIM. Construction professionals resolve these issues on site all the time. Likewise, they will need to make decisions in such situations when using the proposed apparatus. The new system does not introduce any new complexity. On the contrary, it should greatly facilitate identification and resolution of such discrepancies, for two reasons:

a) The apparatus provides richer information about discrepancies than can currently be obtained using traditional tools (such as tape measures) because the scanner measures the as-built dimensions and planes of the room surfaces with high accuracy (< 5 mm).

b) The apparatus delivers the information in a readily interpretable form. It displays the as-designed information directly in the context of the work, making the consequences of any discrepancy quite clear, with no need for the exhaustive

interpretation that is typically required of workers and engineers on site in such situations.

Once a correction decision has been made, a worker could use a system control interface, possibly provided on a hand-held device, to move, rotate or scale a projected image to implement the agreed upon solution. Alternatively, the as-built measurements could be copied into the BIM model, thus enabling designers to resolve the issue, make design corrections to suit real conditions and adjust the model. The new design solution could then be projected, verified and built accordingly to reflect the design intent. The camera could easily be used to communicate issues to designers in their offices; one could even imagine remote designers making adjustments to the projected images in real-time.

Similarly, the development of better prototypes may spawn research into additional novel ways of working with the tool. For example, a system function to photograph images of the work, upload them to the system, and register their location and pose in the BIM model to serve as embedded records of the as-built conditions, might be very useful. It might also be used to project different tiling layouts or other design options for review by customers to select finishes in situ.

VI. Conclusion

In this work, we propose an efficient approach that projects rich information from a BIM model onto the construction surface, directly augmenting the construction site with the design information. This is done using a portable system consisting of LiDAR, an angled adjustable projector, and a camera. The system localizes itself within the already built outer walls using the LiDAR and the BIM model, calibrates the projection correction parameters (keystone correction) using image analysis, and projects the information correctly onto the surface. Testing results showed that the localization had a mean error of about 5 mm, and the final projected image's error was approximately one centimeter. Each time the system is moved by the user, it re-localizes itself in under five seconds and projects the new relevant information. The system automates the layout task, preserves accuracy, and can provide rich model information on any interior surface.

Current efforts to automate the laborious task of marking out construction works bear witness to the widely perceived inadequacy of existing tools for delivering the rich content of BIM models to the construction workface. The basic approach described in this paper holds the potential to deliver full graphic and textual information directly to the precise location in which it is needed and in a format that can be customized to suit the needs of the trade using the tool and the stage in the construction process. It requires no specialist operator and is straightforward to set up and to use.

VII. Acknowledgements

The authors would like to thank Alon Danay for prototype design and for helping with experiments.

References

[1] C. Woodward, T. Kuula, P. Honkamaa, M. Hakkarainen, and P. Kemppi, "Implementation and evaluation of a mobile augmented reality system for building maintenance," in *Proceedings of the 14th International Conference on Construction Applications of Virtual Reality, Dawood N. and Alkass S. (eds.)*, 2014, pp. 306–315.

[2] H.-L. Chi, S.-C. Kang, and X. Wang, "Research trends and opportunities of augmented reality applications in architecture, engineering, and construction," *Autom. Constr.*, vol. 33, pp. 116–122, Aug. 2013.

[3] X. Wang, M. J. Kim, P. E. D. Love, and S.-C. Kang, "Augmented Reality in built environment: Classification and implications for future research," *Autom. Constr.*, vol. 32, pp. 1–13, Jul. 2013.

[4] D. Casale, *Project Lion - A DPR/Trimble Automated Layout Robot*. DPR Construction, 2013.

[5] J. M. Prouty, *Robotic Construction Site Marking Apparatus*. Google Patents, 2013.

[6] Trimble, "Trimble RTS Series Robotic Total Stations." [Online]. Available: http://www.trimble.com/construction/building-construction/RTS-Series-Robotic-Total-Stations.aspx. [Accessed: 16-Aug-2016].

[7] S. Lee and Ö. Akin, "Augmented reality-based computational fieldwork support for equipment operations and maintenance," *Autom. Constr.*, vol. 20, no. 4, pp. 338–352, 2011.

[8] R. Sacks, C. M. Eastman, G. Lee, and P. Teicholz, *BIM Handbook: A Guide to Building Information Modeling for Owners, Designers, Engineers, Contractors, and Facility Managers*, 3rd ed. Hoboken NJ: John Wiley and Sons, 2018.

[9] O. Bimber and R. Raskar, *Spatial Augmented Reality: Merging Real and Virtual Worlds*. CRC press, 2005.

[10] X. Wang, "Improving Human-Machine Interfaces for Construction Equipment Operations with Mixed and Augmented Reality," in *Robotics and Automation in Construction*, Eds. Carlo., InTech, 2008, p. 404.

[11] C. Koch, M. Neges, M. König, and M. Abramovici, "Natural markers for augmented reality-based indoor navigation and facility maintenance," *Autom. Constr.*, vol. 48, pp. 18–30, Dec. 2014.

[12] L. Hou, X. Wang, L. Bernold, and P. Love, "Using Animated Augmented Reality to Cognitively Guide Assembly," *J. Comput. Civ. Eng.*, vol. 27, no. 5, pp. 439–451, 2013.

[13] X. Yang and S. Ergan, "Evaluation of visualization techniques for use by facility operators during monitoring tasks," *Autom. Constr.*, vol. 44, pp. 103–118, Aug. 2014.

[14] S. Meža, Ž. Turk, and M. Dolenc., "Component based engineering of a mobile BIM-based augmented reality system," *Autom. Constr.*, vol. 42, pp. 1–12, Jun. 2014.

[15] X. Wang, M. Truijens, L. Hou, Y. Wang, and Y. Zhou, "Integrating Augmented Reality with Building Information Modeling: Onsite construction process controlling for liquefied natural gas industry," *Autom. Constr.*, vol. 40, pp. 96–105, Apr. 2014.

[16] L. Hou, X. Wang, and M. Truijens, "Using Augmented Reality to Facilitate Piping Assembly: An Experiment-Based Evaluation," *J. Comput. Civ. Eng.*, vol. 29, no. 1, p. 5014007, 2015.

[17] J. Irizarry, M. Gheisari, G. Williams, and B. N. Walker, "InfoSPOT: A mobile Augmented Reality method for accessing building information through a situation awareness approach," *Autom. Constr.*, vol. 33, pp. 11–23, Aug. 2013.

[18] C.-S. Park, D.-Y. Lee, O.-S. Kwon, and X. Wang, "A framework for proactive construction defect management using BIM, augmented reality and ontology-based data collection template," *Autom. Constr.*, vol. 33, pp. 61–71, Aug. 2013.

[19] G. Williams, M. Gheisari, P. Chen, and J. Irizarry, "BIM2MAR: An Efficient BIM Translation to Mobile Augmented Reality Applications," *J. Manag. Eng.*, vol. 31, no. 1, p. A4014009, 2015.

[20] P. Daponte, L. De Vito, F. Picariello, and M. Riccio, "State of the art and future developments of the Augmented Reality for measurement applications," *Measurement*, vol. 57, pp. 53–70, Nov. 2014.

[21] D. H. Shin and P. S. Dunston, "Identification of application areas for Augmented Reality in industrial construction based on technology suitability," *Autom. Constr.*, vol. 17, no. 7, pp. 882–894, 2008.

[22] K. Tanaka, M. Kajitani, C. Kanamori, H. Itoh, Y. Abe, and Y. Tanaka, "Development of Marking Robot Working at Building

Sites," in *Proceedings: ISARC95*, IMBiGS, 1995, pp. 235–242.
[23] J. R. Watts, *Navigating robot with reference line plotter*. Google Patents, 1995.
[24] Theometrics, "TheoBOT," 2010. [Online]. Available: https://www.youtube.com/watch?v=tJ735VaOIqY. [Accessed: 16-Aug-2016].
[25] Y. Rosenfeld and A. Warszawski, "Economic Feasibility of Automation in Building Construction," in *Information Support for Building Economics, CIBW55 Workshop Proceedings*, 1997, pp. 109–124.
[26] F. Dellaert, D. Fox, W. Burgard, and S. Thrun, "Monte carlo localization for mobile robots," in *Robotics and Automation, 1999. Proceedings. 1999 IEEE International Conference on*, vol. 2, IEEE, 1999, pp. 1322–1328.
[27] D. Fox, W. Burgard, and S. Thrun, "Markov localization for mobile robots in dynamic environments," *J. Artif. Intell. Res.*, pp. 391–427, 1999.
[28] R. Sukthankar and M. D. Mullin, "Automatic keystone correction for camera-assisted presentation interfaces," in *Advances in Multimodal Interfaces—ICMI 2000*, Springer, 2000, pp. 607–614.
[29] Y. Okubo, C. Ye, and J. Borenstein, "Characterization of the Hokuyo URG-04LX laser rangefinder for mobile robot obstacle negotiation," in *Proceedings of the SPIE, Volume 7332, id. 733212 (2009).*, 2009, vol. 7332, p. 733212.
[30] J. C. Lee, P. H. Dietz, D. Maynes-Aminzade, R. Raskar, and S. E. Hudson, "Automatic projector calibration with embedded light sensors," in *Proceedings of the 17th annual ACM symposium on User interface software and technology - UIST '04*, 2004, p. 123.
[31] S. Zollmann, T. Langlotz, and O. Bimber, "Passive-Active Geometric Calibration for View-Dependent Projections onto Arbitrary Surfaces," *J. Virtual Real. Broadcast.*, vol. 4, no. 6, 2007.